

Stability and convergence analysis of a domain decomposition FE/FD method for the Maxwell's equations in time domain

M. Asadzadeh* and L. Beilina*

Abstract

Stability and convergence analysis for the domain decomposition finite element/finite difference (FE/FD) method developed in [2, 3] is presented. The analysis is designed for semi-discrete finite element scheme for the time-dependent Maxwell's equations. The explicit finite element schemes in different settings of the spatial domain are constructed and domain decomposition algorithm is formulated. Several numerical examples validate convergence rates obtained in the theoretical studies.

1 Introduction

New computational techniques meet the needs of industry in developing efficient computational methods to simulate partial differential equations (PDEs). Especially, for simulations in higher dimensions and large computational domains. In this regard, certain *domain decomposition* (DD) method leading to efficient schemes, in numerical investigations, has gained a lot of interest in numerical analysis community. This variant of the DD method is the subject of our current, and some related and ongoing, research. This type of schemes was previously studied, e.g. in [11, 29] for others than studied here problems.

The present work is a further development of the DD hybrid finite element/finite difference (FE/FD) method for time-dependent Maxwell's equations for electric field in non-conductive media, studied in [2, 3]. A stable, time-domain (TD), DDM scheme for Maxwell's equations was proposed in [25, 26], and further verified in [12]. This method uses FDTD scheme on the, structured, FD part of the mesh, and edge elements on unstructured part. In applications, because of edge elements implementation, this method remains computationally expensive.

*Department of Mathematical Sciences, Chalmers University of Technology and University of Gothenburg, SE-42196 Gothenburg, Sweden, e-mail: mohammad@chalmers.se, larisa@chalmers.se

The domain decomposition FE/FD method for time-dependent Maxwell's equations for electric field, assuming constant dielectric permittivity function in a finite difference domain, was considered in [2]. This assumption simplifies the numerical schemes in both FE and FD domains and significantly reduces computational efforts for implementation of the whole DD method. Modified numerical scheme, energy estimate and numerical verifications of this method was presented in [3]. However, the fully stability and convergence analysis with numerical implementations, in L_2 - and H^1 -norms of the developed FE and FD schemes, are not presented in the above studies. We fill this gap in the present work.

More specifically, we present stability analysis for explicit schemes for both FEM and FDM in the DD hybrid FE/FD method. The DDM is constructed such that FEM and FDM coincide on the common, structured, overlapping layer between the two subdomains. The resulting domain decomposition approach at the overlapping layers can be viewed as a FE scheme which avoids instabilities at the interfaces. Similar to the DD approach of [3, 4], we decompose the computational domain such that FEM and FDM are used in different subdomains: FDM in simple geometry and FE in the subdomain where more detailed information is needed about the structure of this subdomain. This also allows application of adaptive FEM in such subdomain, see, e.g. [1, 2, 7, 8, 9, 27, 28].

Reliability and convergence of the domain decomposition method, studied in this work, are evident for solution of coefficient inverse problems (CIPs) in \mathbb{R}^3 , see, e.g. [7, 8, 9, 27, 28]. For the case of CIPs, the computational domain is splitted into subdomains such that a simple discretization scheme can be used in a large region and more refined discretization scheme is applied in smaller, however more critical, part of the domain. In most algorithms for solution of electromagnetic CIPs, to determine the dielectric permittivity function inside a computational domain, a qualitative collection of experimental measurements is necessary on it's boundary or in it's neighborhood. In such cases it is convenient to consider the numerical solution of time-dependent Maxwell's equations in different subdomains with constant dielectric permittivity function in some subdomain and non-constant in the other ones. For the time-dependent Maxwell's equations, the DD scheme of [3], which is analyzed in the present work, is used for solution of different CIPs to determine the dielectric permittivity function in non-conductive media using simulated and experimentally generated data, see [1, 7, 8, 9, 27, 28].

An outline of this paper is as follows. In Section 2 we introduce the mathematical model. In Section 3 we briefly present the domain decomposition FE/FD method and communication scheme between two methods. In Section 4 we describe the domain decomposition FE/FD method for solution of Maxwell's equations and set up the finite element and finite difference schemes. Section 5 is devoted to the stability analysis. In Section 6, we derive optimal a priori error estimates in finite element method for the semi-discrete (spatial discretizations) problems. Finally, in Section 7 we present numerical implementations that justify the theoretical investigations of the paper. In what follows, C will be a generic constant independent of all parameters, unless otherwise specifically specified, and not necessarily the same at each occurrence.

2 The mathematical model

The Cauchy problem for the electric field $E(x, t) = (E_1, E_2, E_3)(x, t)$, $x \in \mathbb{R}^3$, $t \in [0, T]$, of the Maxwell's equations, under the assumptions that the dimensionless relative magnetic permeability of the medium is $\mu_r \equiv 1$ and the electric volume charges are zero, is given by

$$\begin{aligned} \frac{1}{c^2} \varepsilon_r(x) \frac{\partial^2 E}{\partial t^2} + \nabla \times \nabla \times E &= -\mu_0 \sigma(x) \frac{\partial E}{\partial t}, \\ \nabla \cdot (\varepsilon E) &= 0, \end{aligned} \quad (1)$$

where, $\varepsilon_r(x) = \varepsilon(x)/\varepsilon_0$ and $\sigma(x)$ are the dimensionless relative dielectric permittivity and electric conductivity functions, respectively. ε_0 , and μ_0 are the permittivity and permeability of the free space, respectively, and $c = 1/\sqrt{\varepsilon_0 \mu_0}$ is the speed of light in free space. In this paper we consider the problem (1) in non-conductive media, i.e. $\sigma \equiv 0$, and hence study the initial value problem

$$\begin{aligned} \varepsilon(x) \frac{\partial^2 E}{\partial t^2} + \nabla \times \nabla \times E &= 0, \quad x \in \mathbb{R}^3, t \in (0, T]. \\ \nabla \cdot (\varepsilon E) &= 0, \\ E(x, 0) = f_0(x), \quad \frac{\partial E}{\partial t}(x, 0) &= f_1(x), \quad x \in \mathbb{R}^3, t \in (0, T]. \end{aligned} \quad (2)$$

To solve the problem (2) numerically, we consider it in a bounded domain $\Omega \subset \mathbb{R}^n$, $n = 2, 3$ (instead of whole \mathbb{R}^n), with boundary $\partial\Omega$, and employ a split scheme on Ω : a hybrid, finite element/finite difference scheme, *kind of* domain decomposition, developed in [2, 3] and summarized in Algorithm 1. More specifically, we divide the computational domain Ω into two subregions, Ω_{FEM} and Ω_{FDM} such that $\Omega = \Omega_{\text{FEM}} \cup \Omega_{\text{FDM}}$ and Ω_{FEM} is a subset of the convex hull of Ω_{FDM} . The function $\varepsilon(x)$ is assumed to be constant in Ω_{FDM} , and bounded and smooth in Ω_{FEM} . The communication β between Ω_{FEM} and Ω_{FDM} is arranged using an overlapping mesh structure through a two-element thick layer around Ω_{FEM} as shown by blue and green common boundaries in Figure 1. The blue boundary is outer boundary of Ω_{FEM} and inner boundary of Ω_{FDM} . Similarly, the green boundary is the inner boundary of Ω_{FEM} from which the solution is copied to the green boundary of Ω_{FDM} .

The key idea with such a decomposition is to be able apply different numerical methods in different computational domains. For the numerical solution of (2) in Ω_{FDM} we use the finite difference method on a structured mesh. In Ω_{FEM} , we use finite elements on a sequence of unstructured meshes $K_h = \{K\}$, with elements K consisting of triangles in \mathbb{R}^2 and tetrahedra in \mathbb{R}^3 , both satisfying minimal angle condition. This approach combines the flexibility of the finite elements and the efficiency of the finite differences in terms of speed and memory usage and fits well for reconstruction algorithms presented below.

We assume that for some known constant $d > 1$, the function $\varepsilon \in C^2(\mathbb{R}^3)$ satisfies

$$\begin{aligned} \varepsilon(x) &\in [1, d], & \text{for } x \in \Omega_{\text{FEM}}, \\ \varepsilon(x) &= 1, & \text{for } x \in \Omega_{\text{FDM}}. \end{aligned} \quad (3)$$

Conditions (3) on ε and the relation

$$\nabla \times \nabla \times E = \nabla(\nabla \cdot E) - \nabla \cdot (\nabla E), \quad (4)$$

together with divergence free field E , make equations in (2) independent of each others in Ω_{FEM} and Ω_{FDM} so that, in Ω_{FDM} , we just need to solve the system of wave equations:

$$\frac{\partial^2 E}{\partial t^2} - \Delta E = 0, \quad (x, t) \in \Omega_2 \times (0, T]. \quad (5)$$

Remark

It is well known that, for stable implementation of the finite element solution of Maxwell's equations, divergence-free edge elements are the most satisfactory ones from a theoretical point of view [20, 23]. However, the edge elements are less attractive for solution of time-dependent problems, since a linear system of equations should be solved at each time iteration step. In contrary, P1 elements can be efficiently used in a fully explicit finite element scheme with lumped mass matrix [10, 13, 17]. It is also well known that numerical solution of Maxwell's equations using nodal finite elements is often unstable and results spurious oscillatory solutions [21, 24]. There are a number of techniques to overcome such instabilities, see, e.g. [14, 15, 16, 22, 24].

In [5, 6], a finite element analysis shows stability and consistency of the stabilized finite element method for the solution of (1) with $\sigma(x) = 0$. In the current study we show stability and convergence for the combined FEM/FDM scheme, under the condition (3) on ε , where the stabilized FEM is used for the numerical solution of (2) in Ω_{FEM} and usual FDM discretization of (5) is applied in Ω_{FDM} .

Remark

Here, we consider the case when $E(x, t) = 0$ for $x \in \partial\Omega$. Further, we assume that $E(x, 0) \in [H^1(\Omega)]^3$, $\frac{\partial E}{\partial t}(x, 0) \in \mathbf{H}(\text{div}, \Omega)$ and $\nabla \cdot (\varepsilon E(x, 0)) = \nabla \cdot (\varepsilon \frac{\partial E}{\partial t}(x, 0)) = 0$. Recall that we assumed non-conductive media: $\sigma \equiv 0$. In the presence of electric conductivity, additional σ -terms appear in the equations. They lead to more involved estimates and heavier implementations which we plan to perform in a forthcoming study.

Hence, in this note we study the following initial boundary value problem:

$$\begin{cases} \varepsilon \partial_{tt} E + \nabla \times \nabla \times E = 0 & \text{in } \Omega \times (0, T), \\ E(\cdot, 0) = f_0(\cdot), \text{ and } \partial_t E(\cdot, 0) = f_1(\cdot) & \text{in } \Omega, \\ E = 0 & \text{on } \partial\Omega \times (0, T), \\ \nabla \cdot (\varepsilon E) = 0 & \text{in } \Omega. \end{cases} \quad (6)$$

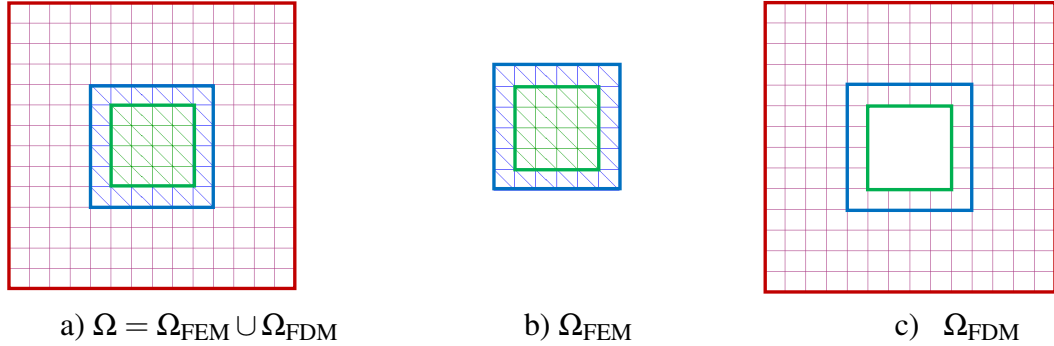


Figure 1: Domain decomposition and mesh discretization in Ω . The mesh of Ω is a combination of the quadrilateral finite difference mesh Ω_{FDM} presented on c), and the finite element mesh Ω_{FEM} presented on b). Domains Ω_{FEM} and Ω_{FDM} overlap by two layers of structured nodes such that they have common boundaries shown by green and blue colors.

3 The structure of domain decomposition

We now describe the DD method between two domains, Ω_{FEM} and Ω_{FDM} , where the FEM is used for computation of the solution in Ω_{FEM} , and FDM is used in Ω_{FDM} . Communication between Ω_{FEM} and Ω_{FDM} is achieved letting overlapping of both meshes across a two-element thick layer around $\partial\Omega_{FEM}$ - see Figure 1. The common nodes of both Ω_{FEM} and Ω_{FDM} domains belong to either of the following boundaries (see Figure 1):

- Nodes on the blue boundary ω_o - lie on the boundary $\partial\Omega_{FEM}$ of Ω_{FEM} and are interior to Ω_{FDM} ,
- Nodes on the green boundary ω_\diamond - lie on the inner boundary $\partial\Omega_{FDM}$ of Ω_{FDM} and are interior to Ω_{FEM} .

Then the main loop in time for the explicit hybrid FEM/FDM scheme, that solves (2) associates with appropriate boundary conditions, at each time step k is described in Algorithm 1 below:

By (3), $\varepsilon = 1$ at the overlapping nodes between Ω_{FEM} and Ω_{FDM} . Thus, FEM and FDM schemes coincide on the common, structured, overlapping layer. Hence, we avoid instabilities at interfaces.

Algorithm 1 Domain decomposition process for hybrid FE/FD scheme

- 1: On the mesh Ω_{FDM} , where FDM is used, update the Finite Difference (FD) solution.
 - 2: On the mesh Ω_{FEM} , where FEM is used, update the Finite Element (FE) solution.
 - 3: Copy FE solution obtained at nodes ω_\circ (nodes on the green boundary of Figure 1) as a boundary condition on the inner boundary for the FD solution in Ω_{FDM} .
 - 4: Copy FD solution obtained at nodes ω_\circ (nodes on the blue boundary of Figure 1) as a boundary condition for the FE solution on $\partial\Omega_{FEM}$ of Ω_{FEM} .
 - 5: Apply boundary condition at $\partial\Omega$ at the red boundary of Ω_{FDM} .
-

4 Derivation of computational schemes

In this section we construct, combined, finite element-finite difference schemes to solve the model problem (6). To do this, first we present the finite element scheme to solve (6) in entire Ω . This induces the finite element scheme in Ω_{FEM} . Then, we derive the finite difference scheme in Ω_{FDM} , when the domain decomposition FE/FD structure is applied to solve (6) in Ω .

Remark

The computational schemes derived in this section are explicit and therefore, for their convergence, the CFL condition below (see ,e.g. [5, 6]) should be satisfied

$$\tau \leq \frac{h}{\eta}, \quad \eta = C\sqrt{1 + 3\|\varepsilon - 1\|_\infty}. \quad (7)$$

Here C is a mesh independent constant, τ is the time step, and h is the mesh size.

In the sequel, we denote the inner product of $[L^2(\Omega)]^M, M \in \{1, 2, 3\}$, by (\cdot, \cdot) , and the corresponding norm by $\|\cdot\|$. The scalar inner product in $[L^2(\Omega_{FEM})]^M$ we denote by $(\cdot, \cdot)_{\Omega_{FEM}}$, and the associated norm by $\|\cdot\|_{\Omega_{FEM}}$. Further, we let $\partial\Omega_{FEM}$ to be the boundary of Ω_{FEM} , $\partial\Omega_{FDM}$ the inner boundary of Ω_{FDM} and $\partial\Omega$ the outer boundary of Ω_{FDM} .

4.1 Finite element discretization in Ω

First we derive finite element scheme to solve the model problem (6) in whole Ω . Next, we discretize $\Omega_{FEM_T} = \Omega_{FEM} \times (0, T)$ in two steps: (i) the spatial discretization using a partition $K_h = \{K\}$ of Ω_{FEM} into elements K , where $h = h(x)$ is a mesh function defined as $h|_K = h_K$, representing the local diameter of elements. We also denote by $\partial K_h = \{\partial K\}$ a partition of the boundary $\partial\Omega_{FEM}$ into boundaries ∂K of the elements K such that, at least one of the vertices of these elements belong to $\partial\Omega_{FEM}$. (ii) As for temporal discretization, we let J_τ be a uniform partition of the time interval $(0, T)$ into N subintervals $J = (t_{k-1}, t_k]$ of length $\tau = T/N$. As usual, we also assume a minimal angle condition on elements K in K_h . To formulate the finite element method for (6) in Ω , we introduce the finite element

space $W_h^E(\Omega)$ for each component of the electric field E defined by

$$W_h^E(\Omega) := \{w \in H^1(\Omega) : w|_K \in P_1(K), \forall K \in K_h\},$$

where $P_1(K)$ denote the set of piecewise-linear functions on K . Setting $\mathbf{W}_h^E(\Omega) := [W_h^E(\Omega)]^3$ we define f_{0h} (resp. f_{1h}) to be the usual \mathbf{W}_h^E -interpolant of f_0 (resp. f_1) in (6). Also, because of the Dirichlet boundary data in (6) we need to choose the test function space as

$$\mathbf{W}_{h,0}^E := \{\mathbf{v} \in \mathbf{W}_h^E | \mathbf{v} = 0, \quad \text{on} \quad \partial\Omega\}. \quad (8)$$

Then, recalling (4), and the fact that $\nabla \cdot (\varepsilon E) = 0$, the spatial semi-discrete problem in Ω reads:

Find $E_h \in \mathbf{W}_h^E(\Omega)$ such that $\forall \mathbf{v} \in \mathbf{W}_{h,0}^E(\Omega)$,

$$\begin{aligned} & (\varepsilon \partial_{tt} E_h, \mathbf{v}) + (\nabla E_h, \nabla \mathbf{v}) + (\nabla \cdot (\varepsilon E_h), \nabla \cdot \mathbf{v}) - (\nabla \cdot E_h, \nabla \cdot \mathbf{v}) \\ & - \langle \partial_n E_h, \mathbf{v} \rangle_{\partial\Omega} := \sum_{j=1}^5 T_j = 0, \\ & E_h(\cdot, 0) = f_{0h}(\cdot) \quad \text{and} \quad \partial_t E_h(\cdot, 0) = f_{1h}(\cdot) \quad \text{in } \Omega. \end{aligned} \quad (9)$$

We note that

$$T_3 = (\nabla \cdot (\varepsilon E_h), \nabla \cdot \mathbf{v}) = (\nabla \varepsilon \cdot E_h, \nabla \cdot \mathbf{v}) + (\varepsilon \nabla \cdot E_h, \nabla \cdot \mathbf{v}),$$

implies that

$$\begin{aligned} T_3 + T_4 &= (\nabla \cdot (\varepsilon E_h), \nabla \cdot \mathbf{v}) - (\nabla \cdot E_h, \nabla \cdot \mathbf{v}) \\ &= (\nabla \varepsilon \cdot E_h, \nabla \cdot \mathbf{v}) + \left((\varepsilon - 1) \nabla \cdot E_h, \nabla \cdot \mathbf{v} \right). \end{aligned} \quad (10)$$

Recalling (8), vanishing test functions at the boundary yields $T_5 \equiv 0$, and the final weak formulation for the semi-discrete problem in Ω is: Find $E_h \in \mathbf{W}_h^E(\Omega)$ such that $\forall \mathbf{v} \in \mathbf{W}_{h,0}^E(\Omega)$,

$$B_\Omega(E_h, \mathbf{v}) := (\varepsilon \partial_{tt} E_h, \mathbf{v}) + (\nabla E_h, \nabla \mathbf{v}) + (\nabla \varepsilon \cdot E_h, \nabla \cdot \mathbf{v}) + ((\varepsilon - 1) \nabla \cdot E_h, \nabla \cdot \mathbf{v}) = 0. \quad (11)$$

For the, reflexive, inhomogeneous boundary condition, see the FE scheme for Ω_{FEM} .

To get fully discrete scheme for (6) we apply time discretization to (9) approximating $E_h(k\tau)$, denoted by E_h^k , where we use the central difference scheme, for $k = 1, \dots, N-1$:

$$\begin{aligned} & \left(\varepsilon \frac{E_h^{k+1} - 2E_h^k + E_h^{k-1}}{\tau^2}, \mathbf{v} \right) + (\nabla E_h^k, \nabla \mathbf{v}) + (\nabla \cdot (\varepsilon E_h^k), \nabla \cdot \mathbf{v}) \\ & - (\nabla \cdot E_h^k, \nabla \cdot \mathbf{v}) = 0 \quad \forall \mathbf{v} \in \mathbf{W}_{h,0}^E(\Omega), \end{aligned} \quad (12)$$

$$E_h^0 = f_{0h} \quad \text{and} \quad E_h^1 = E_h^0 + \tau f_{1h} \quad \text{in } \Omega.$$

Multiplying both sides of (12) by τ^2/ε we get, $\forall \mathbf{v} \in \mathbf{W}_{h,0}^E(\Omega)$, that

$$\begin{aligned} & \left(E_h^{k+1} - 2E_h^k + E_h^{k-1}, \mathbf{v} \right) + \tau^2(1/\varepsilon \nabla E_h^k, \nabla \mathbf{v}) + \tau^2(1/\varepsilon \nabla \cdot (\varepsilon E_h^k), \nabla \cdot \mathbf{v}) \\ & - \tau^2(1/\varepsilon \nabla \cdot E_h^k, \nabla \cdot \mathbf{v}) = 0, \end{aligned} \quad (13)$$

$$E_h^0 = f_{0h} \quad \text{and} \quad E_h^1 = E_h^0 + \tau f_{1h}, \quad \text{in } \Omega.$$

Rearranging terms in (13) we get the following scheme: *Given the approximate initial data, f_{0h} and f_{1h} , find $E_h \in \mathbf{W}_h^E(\Omega)$ such that $\forall \mathbf{v} \in \mathbf{W}_{h,0}^E(\Omega)$,*

$$\begin{aligned} & \left(E_h^{k+1}, \mathbf{v} \right) = \left(2E_h^k, \mathbf{v} \right) - \left(E_h^{k-1}, \mathbf{v} \right) - \tau^2(1/\varepsilon \nabla E_h^k, \nabla \mathbf{v}) - \tau^2(1/\varepsilon \nabla \cdot (\varepsilon E_h^k), \nabla \cdot \mathbf{v}) \\ & + \tau^2(1/\varepsilon \nabla \cdot E_h^k, \nabla \cdot \mathbf{v}) \end{aligned} \quad (14)$$

$$E_h^0 = f_{0h} \quad \text{and} \quad E_h^1 = E_h^0 + \tau f_{1h} \quad \text{in } \Omega.$$

4.2 Finite element discretization in Ω_{FEM}

To solve the model problem (6) via the domain decomposition FE/FD method, we use the split $\Omega = \Omega_{FEM} \cup \Omega_{FDM}$, see Figure 1. Thus in Ω_{FEM} we use FEM to solve the equation

$$\begin{aligned} & \varepsilon \partial_{tt} E + \nabla \times \nabla \times E = 0 && \text{in } \Omega_{FEM} \times (0, T), \\ & E(\cdot, 0) = f_0(\cdot), \text{ and } \partial_t E(\cdot, 0) = f_1(\cdot) && \text{in } \Omega_{FEM}, \\ & \partial_n E = -\partial_t E = g && \text{on } \partial \Omega_{FEM} \times (0, T), \\ & \nabla \cdot (\varepsilon E) = 0 && \text{in } \Omega_{FEM}. \end{aligned} \quad (15)$$

Here, g is the restriction of the solution obtained by the FDM in Ω_{FDM} to $\partial \Omega_{FEM}$ and therefore the test functions are not vanishing at the boundary and hence the term corresponding to T_5 in (9) will be appearing in the weak formulation.

To formulate the finite element method for (15) in Ω_{FEM} , mimicking (9), we introduce the finite element space $W_h^E(\Omega_{FEM})$ for each component of the electric field E defined by

$$W_h^E(\Omega_{FEM}) := \{w \in H^1(\Omega_{FEM}) : w|_K \in P_1(K), \quad \forall K \in K_h\}.$$

Setting $\mathbf{W}_h^E(\Omega_{FEM}) := [W_h^E(\Omega_{FEM})]^3$ we define f_{0h} , f_{1h} , and g_h to be the usual \mathbf{W}_h^E -interpolants of f_0 , f_1 , and g , respectively, in Ω_{FEM} . Then, similar to the FE scheme for Ω , we get the following finite element scheme for Ω_{FEM} : *Given f_{0h} , f_{1h} , and g_h , find $E_h \in \mathbf{W}_h^E(\Omega_{FEM})$ such that*

$$\begin{aligned} & (\varepsilon \partial_{tt} E_h, \mathbf{v}) + (\nabla E_h, \nabla \mathbf{v}) + (\nabla \cdot (\varepsilon E_h), \nabla \cdot \mathbf{v}) - (\nabla \cdot E_h, \nabla \cdot \mathbf{v}) \\ & = \langle g_h, \mathbf{v} \rangle_{\partial \Omega_{FEM}}, \quad \forall \mathbf{v} \in \mathbf{W}_h^E(\Omega_{FEM}) \end{aligned} \quad (16)$$

$$E_h(\cdot, 0) = f_{0h}(\cdot) \quad \text{and} \quad \partial_t E_h(\cdot, 0) = f_{1h}(\cdot) \quad \text{in } \Omega_{FEM}.$$

A corresponding fully discrete problem in Ω_{FEM_T} reads as follows:
 Given $f_{0h}, f_{1h}, g_h, E_h^k$, and E_h^{k-1} ; find E_h^{k+1} such that

$$\begin{aligned} (E_h^{k+1}, \mathbf{v}) &= (2E_h^k, \mathbf{v}) - (E_h^{k-1}, \mathbf{v}) - \tau^2(1/\varepsilon \nabla E_h^k, \nabla \mathbf{v}) \\ &\quad - \tau^2(1/\varepsilon \nabla \cdot (\varepsilon E_h^k), \nabla \cdot \mathbf{v}) + \tau^2(1/\varepsilon \nabla \cdot E_h^k, \nabla \cdot \mathbf{v}) \\ &\quad + \tau^2 \langle g_h/\varepsilon, \mathbf{v} \rangle_{\partial\Omega_{FEM}}, \quad \forall \mathbf{v} \in \mathbf{W}_h^E(\Omega_{FEM_T}) \end{aligned} \quad (17)$$

$$E_h^0 = f_{0h} \quad E_h^1 = E_h^0 + \tau f_{1h} \quad \text{in } \Omega_{FEM_T}.$$

Remark

Note that, in (15), Dirichlet boundary condition $E = g$ can be considered as well.

4.3 Fully discrete FE scheme for the electric field in Ω_T

We expand the functions E_h in terms of the standard continuous piecewise linear functions $\{\varphi_i(x)\}_{i=1}^M$ in space as

$$E_h = \sum_{i=1}^M E_{h_i}(t) \varphi_i(x), \quad (18)$$

where $E_{h_i}(t)$ denote unknown coefficients at $t \in (0, T]$ and the spatial mesh point $x_i \in K_h$. Then, substituting E_h of (18) in (14), and setting $\mathbf{v} = \sum_{j=1}^M \varphi_j(x)$, we obtain the linear system of equations:

$$\begin{aligned} ME_h^{k+1} &= 2ME_h^k - ME_h^{k-1} - \tau^2 G_1 E_h^k - \tau^2 G_2 E_h^k \\ &\quad + \tau^2 G_3 E_h^k + \tau^2 M_{\partial K} E_h^k. \end{aligned} \quad (19)$$

Note that, unlike (14), now the contributions at boundary of the element appear in $M_{\partial K}$. Here, $M, M_1, M_2, M_{\partial K}$ are the block mass matrices in space, G_1, G_2, G_3 are the block stiffness matrices in space, E_h^k denote the nodal values of $E_h(\cdot, t_k)$, and τ is a uniform time step. Now we define the mapping F_K from the reference element \hat{K} onto K such that $F_K(\hat{K}) = K$ and let $\hat{\varphi}$ be the piecewise linear local basis function on \hat{K} such that $\varphi \circ F_K = \hat{\varphi}$. Then, the explicit formulas for the entries in system of equations (19), for each element K , can be

written as:

$$\begin{aligned}
M_{i,j}^K &= (\varphi_i(x) \circ F_K, \varphi_j(x) \circ F_K)_K, \\
M_{i,j}^{\partial K} &= \left\langle \frac{1}{\varepsilon} \partial_n \varphi_i(x) \circ F_K, \varphi_j(x) \circ F_K \right\rangle_{\partial K}, \\
G_{1,i,j}^K &= \left(\frac{1}{\varepsilon} \nabla \varphi_i \circ F_K, \nabla \varphi_j \circ F_K \right)_K, \\
G_{2,i,j}^K &= \left(\frac{1}{\varepsilon} \nabla \cdot (\varepsilon \varphi_i) \circ F_K, \nabla \cdot \varphi_j \circ F_K \right)_K, \\
G_{3,i,j}^K &= \left(\frac{1}{\varepsilon} \nabla \cdot \varphi_i \circ F_K, \nabla \cdot \varphi_j \circ F_K \right)_K,
\end{aligned} \tag{20}$$

where $(\cdot, \cdot)_K$, and $\langle \cdot, \cdot \rangle_{\partial K}$, denote the $L_2(K)$, and $L_2(\partial K)$, scalar products on K and ∂K , respectively. Note that here ∂K is only the part of the boundary of element K that lies at $\partial\Omega_{FEM}$.

To obtain fully explicit scheme we approximate M with the lumped mass matrix M^L , (see [13, 17, 5] for the details corresponding to the Maxwell's system (2)). Next, we multiply (20) by $(M^L)^{-1}$, and get the following explicit, fully discrete method in Ω :

$$\begin{aligned}
E_h^{k+1} &= 2E_h^k - E_h^{k-1} - \tau^2 (M^L)^{-1} G_1 E_h^k - \tau^2 (M^L)^{-1} G_2 E_h^k \\
&\quad + \tau^2 (M^L)^{-1} G_3 E_h^k + \tau^2 (M^L)^{-1} M_{\partial K} E_h^k.
\end{aligned} \tag{21}$$

4.4 Fully discrete scheme for the electric field in Ω_{FEM_T}

As in the fully discrete FE scheme (19) in Ω_T , we obtain fully discrete FE scheme in Ω_{FEM_T} in the domain decomposition setting: Expanding the E_h functions of Ω_{FEM} via the continuous piecewise linear functions in space as in (18), and then substituting them in (17), (with $\mathbf{v} = \sum_{j=1}^M \varphi_j(x)$, $x \in \Omega_{FEM}$, and $x_i \in K_h \subset \Omega_{FEM}$), we get the linear system of equations:

$$\begin{aligned}
ME_h^{k+1} &= 2ME_h^k - ME_h^{k-1} - \tau^2 G_1 E_h^k - \tau^2 G_2 E_h^k \\
&\quad + \tau^2 G_3 E_h^k + \tau^2 S_{\partial K}.
\end{aligned} \tag{22}$$

Here, M is the block mass matrices in space, restricted to Ω_{FEM} , otherwise the same as in (19), G_1, G_2, G_3 are the block stiffness matrices in space as in (19), $S_{\partial K}$ is the assembled load vector, E_h^k denote the nodal values of $E_h(\cdot, t_k)$, τ is the time step. All quantities are for Ω_{FEM_T} . Defining the mapping F_K for the reference element \hat{K} in the mesh K_h generated in Ω_{FEM} as in the previous section, the formulas for entries of all matrices in the system (22) are the same as those in (20), and the entries of load vector are computed as

$$S_j^K = \left(\frac{g_h}{\varepsilon}, \varphi_j \circ F_K \right)_{\partial K}. \tag{23}$$

Again, approximating M with the lumped mass matrix M^L , we obtain the following fully explicit scheme:

$$\begin{aligned} E_h^{k+1} = & 2E_h^k - E_h^{k-1} - \tau^2(M^L)^{-1}G_1E_h^k - \tau^2(M^L)^{-1}G_2E_h^k \\ & + \tau^2(M^L)^{-1}G_3E_h^k + \tau^2(M^L)^{-1}S_{\partial K}. \end{aligned} \quad (24)$$

4.5 Finite difference formulation

We recall now that from conditions (3) it follows that in Ω_{FDM} the function $\varepsilon(x) = 1$. This means that in Ω_{FDM} for the model problem (2) the forward problem will be

$$\frac{\partial^2 E}{\partial t^2} - \Delta E = 0 \quad \text{in } \Omega_{FDM} \times (0, T), \quad (25)$$

$$E(x, 0) = f_0(x), \quad E_t(x, 0) = f_1(x) \quad \text{in } \Omega_{FDM}, \quad (26)$$

$$E = 0 \quad \text{on } \partial\Omega \times (0, T), \quad (27)$$

$$\partial_n E = \partial_n E_{FEM} \quad \text{on } \partial\Omega_{FDM} \times (0, T). \quad (28)$$

Using standard finite difference discretization of the equation (25) in Ω_{FDM} we obtain the following explicit scheme for the solution of the forward problem:

$$E_{l,j,m}^{k+1} = \tau^2 \Delta E_{l,j,m}^k + 2E_{l,j,m}^k - E_{l,j,m}^{k-1}. \quad (29)$$

In the system of, equations above, $E_{l,j,m}^k$ is the solution at the time iteration k at the discrete point (l, j, m) , τ is the time step, and $\Delta E_{l,j,m}^k$ is the discrete Laplacian.

Note that, in (29), the Dirichlet boundary conditions $E = E_{FEM}$ can be considered as well.

5 Stability

In this section we derive stability estimates for the semi-discrete approximations. For stability in Ω these estimates are extensions of the stability approach derived for the continuous problem in [3]. As for the stability in Ω_{FEM} we get slightly different norms involving contributions corresponding to the reflexive boundary: $\partial\Omega_{FEM}$. We use discrete version of a triple norm induced by the weak variational formulation of (6), where we use the relation (10) (which is not necessary in the continuous case where $\nabla \cdot (\varepsilon E) = 0$, however, in general $\nabla \cdot (\varepsilon E_h) \neq 0$):

Find $E \in \mathbf{W}^E(\Omega)$ such that

$$(\varepsilon \partial_{tt} E, \mathbf{v}) + (\nabla E, \nabla \mathbf{v}) + ((\nabla \varepsilon) \cdot E, \nabla \cdot \mathbf{v}) + ((\varepsilon - 1) \nabla \cdot E, \nabla \cdot \mathbf{v}) = 0, \quad \forall \mathbf{v} \in \mathbf{W}_0^E(\Omega)$$

$$E(\cdot, 0) = f_0(\cdot) \quad \text{and} \quad \partial_t E(\cdot, 0) = f_1(\cdot) \quad \text{in } \Omega.$$

(30)

Remark

In general, in non-divergent free case, the bilinear form induced by (30) is not coercive. Further $H^1(\Omega)$ -conforming finite element may result in spurious solutions. A remedy is through modifying the equation by adding a gauge constrain of Coulomb-type, see, e.g. [20] and [22]. This is supplied by the "zero"-term: $\nabla \cdot (\varepsilon E) = 0$, in (6), which we add in the continuous variational formulation in (9). This, however, is not necessarily true in the discrete forms, e.g. in (16), where most likely $\nabla \cdot (\varepsilon E_h) \neq 0$. Taking $\mathbf{v} = \partial_t E$ in (30), (we used the boundary condition $E = 0$ on $\partial\Omega$), yields

$$\begin{aligned} (\varepsilon \partial_{tt} E, \partial_t E) + (\nabla E, \nabla \partial_t E) + ((\nabla \varepsilon) \cdot E, \nabla \cdot \partial_t E) \\ + ((\varepsilon - 1) \nabla \cdot E, \nabla \cdot \partial_t E) \equiv 0, \end{aligned} \quad (31)$$

which, due to the fact that ε is independent of t , can be rewritten as

$$\begin{aligned} \frac{1}{2} \frac{d}{dt} (\varepsilon \partial_t E, \partial_t E) + \frac{1}{2} \frac{d}{dt} (\nabla E, \nabla E) + ((\nabla \varepsilon) \cdot E, \nabla \cdot \partial_t E) \\ + \frac{1}{2} \frac{d}{dt} ((\varepsilon - 1) \nabla \cdot E, \nabla \cdot E) = 0. \end{aligned} \quad (32)$$

Proposition [3]

Let $\Omega \subset \mathbb{R}^n$, $n = 2, 3$ be a bounded domain with piecewise linear boundary $\partial\Omega$. Then, the equation (6) has a unique solution $E \in H^2(\Omega_T)$. Further Let $f_1 \in L^2_\varepsilon(\Omega)$ and $f_0 \in H^1(\Omega) \cap H^1_{\varepsilon-1}(\Omega)$, then there is a constant $C_\varepsilon^t = C(\|\varepsilon\|, t)$ such that, $\forall t \in (0, T]$, the following stability estimate holds true

$$\begin{aligned} \| \|E\| \|_\varepsilon^2 := \|\partial_t E\|_\varepsilon^2(t) + \|\nabla E\|^2(t) + \|\nabla \cdot E\|_{\varepsilon-1}^2(t) \\ \leq C_\varepsilon^t \left(\|f_1\|_\varepsilon^2 + \|\nabla f_0\|^2 + \|f_0\|^2 + \|\nabla \cdot f_0\|_{\varepsilon-1}^2 \right). \end{aligned} \quad (33)$$

Proof. The estimate (33) is proved in [3], Theorem 4.1 by setting $s = 1$ and $j \equiv 0$. Integrating (33) over the time interval $(0, t]$ we get the desired result. We omit the details. \square

Below we translate this stability to the semi-discrete problem.

5.1 Stability estimate for the semi-discrete problem in Ω

The stability for the semi-discrete problem in Ω is basically as in the continuous case above where all E :s are replaced by E_h with some relevant assumptions in the discrete data, viz.

Lemma

Assume that the interpolants of the data f_0 and f_1 : $f_{0,h}$ and $f_{1,h}$ satisfy the regularity conditions $f_{1,h} \in L^2_\varepsilon(\Omega)$ and $f_{0,h} \in H^1(\Omega) \cap H^1_{\varepsilon-1}(\Omega)$, then for each $t \in (0, T]$

$$\| \|E_h\| \|_\varepsilon^2(t) \leq C_\varepsilon^t \left(\|f_{1,h}\|_\varepsilon^2 + \|\nabla f_{0,h}\|^2 + \|f_{0,h}\|^2 + \|\nabla \cdot f_{0,h}\|_{\varepsilon-1}^2 \right). \quad (34)$$

where

$$\| \|E_h\| \|_\varepsilon^2(t) := \|\partial_t E_h\|_\varepsilon^2(t) + \|\nabla E_h\|^2(t) + \|\nabla \cdot E_h\|_{\varepsilon-1}^2(t). \quad (35)$$

5.2 Stability of the semi-discrete problem in Ω_{FEM}

The stability of the semi-discrete problem in Ω_{FEM} , relying on the variational formulation (16), and due to the appearance of the data function g , is slightly different from (34). We rewrite (16), in view of (10), and with $\mathbf{v} = \mathbf{v}_h = \partial_t E_h$ as: Given $E_h(\cdot, 0) = f_{0h}$, $\partial_t E_h(\cdot, 0) = f_{1h}$, and g_h , find $E_h \in \mathbf{W}_h^E(\Omega_{FEM})$ such that

$$\begin{aligned} (\varepsilon \partial_{tt} E_h, \partial_t E_h) + (\nabla E_h, \nabla \partial_t E_h) + ((\nabla \varepsilon) \cdot E_h, \nabla \cdot \partial_t E_h) \\ + ((\varepsilon - 1) \nabla \cdot E_h, \nabla \cdot \partial_t E_h) = \langle g_h, \partial_t E_h \rangle_{\partial \Omega_{FEM}}. \end{aligned} \quad (36)$$

To deal with the $(\nabla \varepsilon) \cdot E_h$ -term we rewrite (36) in its original form as (9) for Ω_{FEM} and with $\mathbf{v} = \partial_t E_h$:

$$\begin{aligned} (\varepsilon \partial_{tt} E_h, \partial_t E_h) + (\nabla E_h, \nabla \partial_t E_h) + (\nabla \cdot (\varepsilon E_h), \nabla \cdot \partial_t E_h) \\ - (\nabla \cdot E_h, \nabla \cdot \partial_t E_h) = \langle g_h, \partial_t E_h \rangle_{\partial \Omega_{FEM}}. \end{aligned} \quad (37)$$

Once again, in view of Theorem 4.1 in [3], as in the case of stability in Ω , we end up with the following time derivative form in $L_2(\Omega_{FEM})$ norms:

$$\begin{aligned} \frac{1}{2} \frac{d}{dt} \left(\|\partial_t E_h\|_{\varepsilon}^2 + \|\nabla E_h\|^2 + \|E_h\|^2 + \|\nabla \cdot E_h\|_{\varepsilon-1}^2 \right) + \\ \leq \frac{1}{2} \|g_h\|_{\partial \Omega_{FEM}}^2 + \frac{1}{2} \|\partial_t E_h\|_{\partial \Omega_{FEM}}^2. \end{aligned} \quad (38)$$

Hence, integrating (38) over the time interval $(0, t)$, we get $\forall t \in [0, T]$,

$$\begin{aligned} |||E_h|||_{\varepsilon}^{2, FEM}(t) &:= \left(\|\partial_t E_h\|_{\varepsilon}^2 + \|\nabla E_h\|^2 + \|E_h\|^2 + \|\nabla \cdot E_h\|_{\varepsilon-1}^2 \right)(t) \\ &\leq \left(\|\partial_t E_h\|_{\varepsilon}^2 + \|\nabla E_h\|^2 + \|E_h\|^2 + \|\nabla \cdot E_h\|_{\varepsilon-1}^2 \right)(0) \\ &\quad + \int_0^t \|g_h\|_{\partial \Omega_{FEM}}^2 + \int_0^t \|\partial_t E_h\|_{\partial \Omega_{FEM}}^2. \end{aligned} \quad (39)$$

Remark

We don't have electric conductivity: σ -term on the right hand side here. With the presence of σ as in (6), the associated assumptions are $\sigma(x) \geq 1$ in Ω_{IN} and $\sigma(x) = 0$ for $x \in \Omega_2 \cup \Omega_{OUT}$. As for the boundary terms, we may either use trace theorem and hide the $\partial \Omega_{FEM}$ -terms in $|||E_h|||_{\varepsilon}^{FEM}$ in (39), or redefine a modified version of $|||E_h|||_{\varepsilon}^{FEM}$ adding terms corresponding to contributions from the boundary boundary. For the sake of generality we keep the two integrals as is and assume, for the boundary data, $\partial_t E_h \in L_2(\partial \Omega_{FEM})$. Summing up we have the following stability estimate for the semi-discrete problem in Ω_{FEM} :

Lemma

Under the following regularity assumptions on the interpolants for initial conditions: $f_{1,h} \in L^2_\varepsilon(\Omega_{FEM})$, $f_{0,h} \in H^1(\Omega_{FEM})$, $\nabla \cdot f_{0,h} \in L^2_{\varepsilon^{-1}}(\Omega_{FEM})$, and with both boundary data: g_h , and $\partial_t E_h \in L_1\left((0, T); L_2(\partial\Omega_{FEM})\right)$, we have, for all $t \in (0, T]$, the following stability estimate for the semi-discrete Ω_{FEM} problem

$$\begin{aligned} |||E_h|||_\varepsilon^{2,FEM}(t) &\leq \left(\|f_{1,h}\|_\varepsilon^2 + \|\nabla f_{0,h}\|^2 + \|f_{0,h}\|^2 + \|\nabla \cdot f_{0,h}\|_{\varepsilon^{-1}}^2 \right)(0) \\ &\quad + \int_0^t \|g_h\|_{\partial\Omega_{FEM}}^2 + \int_0^t \|\partial_t E_h\|_{\partial\Omega_{FEM}}^2. \end{aligned} \quad (40)$$

Corollary

We could write the right hand side in (36) as $(g_h, \sqrt{\varepsilon} \partial_t E_h / \sqrt{\varepsilon})_{\partial\Omega_{FEM}}$. Then letting $C_{f_0, f_1}^2 := \left(\|f_{1,h}\|_\varepsilon^2 + \|\nabla f_{0,h}\|^2 + \|f_{0,h}\|^2 + \|\nabla \cdot f_{0,h}\|_{\varepsilon^{-1}}^2 \right)(0)$, the inequality (40) can be rewritten as

$$|||E_h|||_\varepsilon^{2,FEM}(t) \leq C_{f_0, f_1}^2 + \int_0^t \|g_h\|_{\partial\Omega_{FEM}}^2 + \int_0^t \left\| \frac{1}{\sqrt{\varepsilon}} \partial_t E_h \right\|_{\varepsilon, \partial\Omega_{FEM}}^2. \quad (41)$$

Thus by the definition of the triple norm and using Cauchy-Schwarz, Poincare and Grönwall's inequalities

$$\|E_h\|_{\varepsilon, \partial\Omega_{FEM}} \leq \|\partial_t E_h\|_{\varepsilon, \partial\Omega_{FEM}} \leq C \left(C_{f_0, f_1} + \int_0^t \|g_h\|_{\partial\Omega_{FEM}} \right) e^{T/\|\sqrt{\varepsilon}\|}. \quad (42)$$

In a similar way one may derive estimates of the gradient (∇E_h) -terms in the triple norm using the trace theorem, viz.

$$\begin{aligned} \left\| \frac{1}{\sqrt{\varepsilon}} \partial_t E_h \right\|_{\varepsilon, \partial\Omega_{FEM}}^2 &\leq \sqrt[4]{8} \left\| \frac{1}{\sqrt{\varepsilon}} \partial_t E_h \right\|_{\varepsilon, \Omega_{FEM}} \left\| \frac{1}{\sqrt{\varepsilon}} \partial_t E_h \right\|_{\varepsilon, W_2^1(\Omega_{FEM})} \\ &\leq \frac{\sqrt[4]{8}}{2} \left\| \frac{1}{\sqrt{\varepsilon}} \partial_t E_h \right\|_{\varepsilon, \Omega_{FEM}}^2 + \frac{\sqrt[4]{8}}{2} \left\| \frac{1}{\sqrt{\varepsilon}} \partial_t E_h \right\|_{\varepsilon, W_2^1(\Omega_{FEM})}^2. \end{aligned} \quad (43)$$

Now since both $\frac{1}{2}\sqrt[4]{8} < 1$ likewise $1/\sqrt{\varepsilon} < 1$ ($\varepsilon > 1$) contributions from the right hand side terms can be hidden in corresponding terms of the triple norm, thus ending up with function and gradient terms estimates with bounds depending on given parameters and functions $\sim \mathcal{M}(C_{f_0, f_1}, g_h, T, \varepsilon)$. We omit the details.

6 Error estimates: Semi-Discrete (SD) problems

In what follows, and for future use in our model problems, we shall assume that $\partial_n E = -\partial_t E$ on $\partial\Omega$, which has the common value g on $\partial\Omega_{FEM}$. Let now $\tilde{E}_h \in \mathbf{W}_h^E(\tilde{\Omega})$, with $\tilde{\Omega} = \Omega$ or $\tilde{\Omega} = \Omega_{FEM}$, be an spatial interpolant of the exact electric field E and set

$$e := E - E_h = (E - \tilde{E}_h) + (\tilde{E}_h - E_h) := \eta + \xi. \quad (44)$$

Then, assuming certain regularity of the data set, and with $\tilde{E} \in \mathbf{W}^E(\tilde{\Omega}) \cap H^s(\tilde{\Omega})$, and with the spectral order $p \sim s \geq 1$, we can prove error estimates of the form

$$[\|e\|]_{\tilde{\Omega}} \leq Ch^p \sim Ch^s, \quad \text{for } \tilde{\Omega} = \Omega \quad \text{or} \quad \tilde{\Omega} = \Omega_{FEM}. \quad (45)$$

In this section, and to make a direct error estimate approach, without relying on the stability norm defined in [3], we use the equivalent norm $[\|\cdot\|]_{\tilde{\Omega}}$, slightly different from the norm in (33), (see the term $\|u\|_{|\nabla \varepsilon|}^2$), and directly obtained from the equation (11):

$$[\|u\|]_{\tilde{\Omega}}^2 := \|\partial_t u\|_{\tilde{\varepsilon}}^2 + \|\nabla u\|^2 + \|u\|_{|\nabla \varepsilon|}^2 + \|\nabla \cdot u\|_{|\nabla \varepsilon| + \varepsilon - 1}^2, \quad \tilde{\Omega} = \Omega \quad \text{or} \quad \tilde{\Omega} = \Omega_{FEM}. \quad (46)$$

Further, by the coercivity modification, see e.g. [20], there is a constant C_ε such that

$$[\|u\|]_{\tilde{\Omega}}^2 \sim \|u\|_{\tilde{\Omega}}^2 \leq C_\varepsilon B_{\tilde{\Omega}}(u, u), \quad \tilde{\Omega} = \Omega \quad \text{or} \quad \tilde{\Omega} = \Omega_{FEM}. \quad (47)$$

Finally

$$[\|u\|]_{\Omega_T}^2 := \int_0^T [\|u\|]_{\tilde{\Omega}}^2 ds, \quad \Omega_T = \Omega \times [0, T] \quad \text{or} \quad \Omega_T = \Omega_{FEM} \times [0, T], \quad (48)$$

likewise

$$[\|u\|]_{\Omega_T}^2 := \int_0^T [\|u\|]_{\tilde{\Omega}}^2 ds, \quad \Omega_T = \Omega \times [0, T] \quad \text{or} \quad \Omega_T = \Omega_{FEM} \times [0, T]. \quad (49)$$

Remark

The original problem, with the presence of the electric conductivity term : $\sigma \partial_t E$ ($\sigma \neq 0$) on the right hand side, would behave as of parabolic type, (actually, quasi-parabolic, due to the presence of $\partial_{tt} E$ -term). Then in (45), and for $E \in H^s(\tilde{\Omega})$, $p \sim s$. But in our current consideration $\sigma \equiv 0$, and the problem is viewed as a system of wave equations (componentwise for E:s) and hence hyperbolic. On the other hand finite elements for the scalar (non-system) hyperbolic problems has been considered in various studies by several authors, showing that the best convergence one can hope is obtained using, e.g. discontinuous Galerkin (see [19]), which yields

$$[\|e\|]_{\tilde{\Omega}} \leq Ch^{s-\theta}, \quad \text{for } \tilde{\Omega} = \Omega \quad \text{or} \quad \Omega_{FEM}, \quad (50)$$

instead of (45) and with $\theta = 1/2$, whereas the finite difference approach for the same, hyperbolic type, problem is more accurate and satisfies (45).

Below we use the very similar argument to derive (45) for the spatial domains Ω and Ω_{FEM} .

6.1 Error estimates: SD problem in Ω

Theorem

For $E \in \mathbf{W}^2(\Omega)$ and continuous piecewise polynomial approximation, assuming

$$\|f_1\|_{L^2_{\varepsilon}(\Omega)}^2 + \|f_0\|_{H^1(\Omega)}^2 + \|f_0\|_{|\nabla\varepsilon|+\varepsilon-1}^2(\Omega) + \|f_0\|_{H^1_{\varepsilon-1}(\Omega)}^2 \leq C,$$

then there is a constant C such that

$$[\|e\|] \leq Ch, \quad (51)$$

Proof. We start with the straightforward estimate for η in (44), using interpolation error:

$$\|u - u_h^I\|_{L_2(\Omega)} \leq C_I \|h \nabla u\|_{L_2(\Omega)}. \quad (52)$$

Note that if $u \in C^2(\Omega)$, then the continuous interpolation, (52) is improved, and

$$\|u - u_h^I\|_{L_2(\Omega)} \leq C_I h^2 \|D_x^2 u\|.$$

However, such improvement can not survive, e.g. in approximating with discontinuous interpolation where jump terms $\left[\frac{\partial u_h}{\partial n}\right]$ are introduced in the outward normal directions to elements, and

$$D_x^2 u \leq \frac{\left[\frac{\partial u_h}{\partial n}\right]}{h}.$$

Consequently, returning to (52) we get:

$$\|u - u_h^I\|_{L_2(\Omega)} \leq C_I h \left\| \left[\frac{\partial u_h}{\partial n}\right] \right\|.$$

Hence, we have the following estimate for the interpolation error:

$$\begin{aligned} [\|\eta\|]_{\varepsilon}^2(t) &= [\|E - \tilde{E}_h\|]_{\varepsilon}^2 = \|\partial_t(E - \tilde{E}_h)\|_{\varepsilon}^2 + \|\nabla(E - \tilde{E}_h)\|^2 \\ &\quad + \|E - \tilde{E}_h\|_{|\nabla\varepsilon|}^2 + \|\nabla \cdot (E - \tilde{E}_h)\|_{(|\nabla\varepsilon|+\varepsilon-1)}^2 \\ &\leq h^2 \left(\|\partial_t E\|_{\varepsilon}^2 + \|\nabla E\|^2 + \|E\|_{|\nabla\varepsilon|}^2 + \|\nabla \cdot E\|_{|\nabla\varepsilon|+\varepsilon-1}^2 \right)(t) \leq (C_{\varepsilon}^t)^2 h^2, \end{aligned} \quad (53)$$

where the last two inequalities are just the consequences of the interpolation error and regularity of the exact solution, respectively. So that we can deduce that the interpolation error is:

$$[\|\eta\|]_{\varepsilon}(c) \sim C_{\varepsilon}^t h. \quad (54)$$

To proceed further we assume continuous variational formulation, i.e. the continuous version of (11):

$$0 = B_{\Omega}(E, \mathbf{v}) = 0 \quad \forall \mathbf{v} \in \mathbf{W}_h^E(\Omega).$$

Hence we can write for $\xi = \tilde{E}_h - E_h$

$$B_\Omega(\xi, \xi) = B_\Omega(\tilde{E}_h - E_h, \xi) = B_\Omega(\tilde{E}_h, \xi) = B_\Omega(E - \tilde{E}_h, \xi) = B_\Omega(\eta, \xi) \quad (55)$$

and hence, in a time interval $(0, t) \subset (0, T)$ we have

$$[\|\xi\|]_\varepsilon^2 = [\|\tilde{E}_h - E_h\|]_\varepsilon^2 \leq C_\varepsilon \int_0^t B_\Omega(\xi, \xi) dt = C_\varepsilon \int_0^t B_\Omega(\eta, \xi) dt, \quad (56)$$

where

$$\begin{aligned} B_\Omega(\eta, \xi) &= (\varepsilon \eta_{tt}, \xi) + (\nabla \eta, \nabla \xi) + ((\nabla \varepsilon) \cdot \eta, \nabla \cdot \xi) \\ &\quad + \left((\varepsilon - 1) \nabla \cdot \eta, \nabla \cdot \xi \right) := \sum_{k=1}^4 J_k(t). \end{aligned} \quad (57)$$

We estimate each $\int_0^t J_k(s) ds$, for $k = 1, 2, 3, 4$, separately. As for J_1 , partial integration, with zero boundary condition, yields

$$\begin{aligned} \int_0^t J_1(s) ds &= \int_0^t (\varepsilon \eta_{ss}, \xi) ds = - \int_0^t (\sqrt{\varepsilon} \eta_s, \sqrt{\varepsilon} \xi_s) ds \\ &\leq \int_0^t \|\eta_s\|_\varepsilon^2 ds + \frac{1}{4} \int_0^t \|\xi_s\|_\varepsilon^2 ds. \end{aligned} \quad (58)$$

Direct estimates for J_2, J_3 (with some formal manipulations), and J_4 -terms give

$$\int_0^t J_2(s) ds = \int_0^t (\nabla \eta, \nabla \xi) \leq \int_0^t \|\nabla \eta\|^2 ds + \frac{1}{4} \int_0^t \|\nabla \xi\|^2 ds, \quad (59)$$

$$\int_0^t J_3(s) ds = \int_0^t ((\nabla \varepsilon) \cdot \eta, \nabla \cdot \xi) \leq \int_0^t \|\eta\|_{|\nabla \varepsilon|}^2 ds + \frac{1}{4} \int_0^t \|\nabla \cdot \xi\|_{|\nabla \varepsilon|}^2 ds, \quad (60)$$

$$\begin{aligned} \int_0^t J_4(s) ds &= \int_0^t \left((\varepsilon - 1) \nabla \cdot \eta, \nabla \cdot \xi \right) ds = \int_0^t (\sqrt{\varepsilon - 1} \nabla \cdot \eta, \sqrt{\varepsilon - 1} \nabla \cdot \xi) ds \\ &\leq \int_0^t \|\nabla \cdot \eta\|_{\varepsilon - 1}^2 ds + \frac{1}{4} \int_0^t \|\nabla \cdot \xi\|_{\varepsilon - 1}^2 ds. \end{aligned} \quad (61)$$

Thus by a kick back argument all ξ -norms on the right hand side, can be hidden in the corresponding terms in $[\|\xi\|]_\varepsilon^2$ leading to a η estimate for ξ :

$$[\|\xi\|]_\varepsilon(t) \leq C_\varepsilon [\|\eta\|]_\varepsilon(t). \quad (62)$$

Now, recalling (54) we get the desired result. \square

Proposition

With the same assumption as in the theorem 6.1 above we have the convergence rate of the time derivative e_t for the error:

$$[\|e_t\|]_\varepsilon(t) \leq C_\varepsilon^t h. \quad (63)$$

Proof. Evidently the interpolation estimates in the proof of theorem 6.1 also yield for η_t , and

$$[\|\eta_t\|]_\varepsilon(t) \leq C_\varepsilon^t h. \quad (64)$$

Note that we have no time discretization yet. The remaining step is to show that

$$[\|\xi_t\|]_\varepsilon(t) \leq C_\varepsilon^t [\|\eta_t\|]_\varepsilon(t). \quad (65)$$

The same procedure with η and ξ replaced by η_t and ξ_t , respectively, yields

$$\begin{aligned} B_\Omega(\xi_t, \partial_t \xi) &= B_\Omega((\tilde{E}_h - E_h)_t, \partial_t \xi) = B_\Omega(\tilde{E}_{h,t}, \partial_t \xi) \\ &= B_\Omega((E - \tilde{E}_h)_t, \partial_t \xi) = B_\Omega(\eta_t, \partial_t \xi) \end{aligned} \quad (66)$$

and hence

$$[\|\xi_t\|]_\varepsilon^2 = [\|\partial_t(\tilde{E}_h - E_h)\|]_\varepsilon^2 \leq C_\varepsilon^t \int_0^T B_\Omega(\xi_t, \xi_t) dt = C_\varepsilon^t \int_0^T B_\Omega(\eta_t, \xi_t) dt, \quad (67)$$

where

$$\begin{aligned} B_\Omega(\eta_t, \partial_t \xi) &= (\varepsilon \eta_{ttt}, \xi_t) + (\nabla \eta_t, \nabla \xi_t) + ((\nabla \varepsilon) \cdot \eta_t, \nabla \cdot \xi_t) \\ &\quad + \left((\varepsilon - 1) \nabla \cdot \eta_t, \nabla \cdot \xi_t \right) := \sum_{k=1}^4 I_k(t). \end{aligned} \quad (68)$$

Mimiking the above procedure we estimate $\int_0^t I_k(s) ds$ -terms for $k = 1, 2, 3, 4$, viz.

$$\begin{aligned} \int_0^t I_1(s) ds &= \int_0^t (\varepsilon \eta_{sss}, \xi_s) ds = - \int_0^t (\sqrt{\varepsilon} \eta_{ss}, \sqrt{\varepsilon} \xi_{ss}) ds \\ &\quad + \varepsilon \eta_{ss}(t) \xi_s(t) - \varepsilon \eta_{ss}(0) \xi_s(0) \leq \int_0^t \|\eta_{ss}\|_\varepsilon^2 ds + \frac{1}{4} \int_0^t \|\xi_{ss}\|_\varepsilon^2 ds, \end{aligned} \quad (69)$$

where, with the continuous in time, the spatial discrete errors for η_{ss} and ξ_s are assumed to be zero for all $t \in [0, T]$.

$$\int_0^t I_2(s) ds = \int_0^t (\nabla \eta_s, \nabla \xi_s) \leq \int_0^t \|\nabla \eta_s\|^2 ds + \frac{1}{4} \int_0^t \|\nabla \xi_s\|^2 ds, \quad (70)$$

$$\int_0^t I_3(s) ds = \int_0^t ((\nabla \varepsilon) \cdot \eta_s, \nabla \cdot \xi_s) \leq \int_0^t \|\eta_s\|_{|\nabla \varepsilon|}^2 ds + \frac{1}{4} \int_0^t \|\nabla \cdot \xi_s\|_{|\nabla \varepsilon|}^2 ds, \quad (71)$$

$$\begin{aligned}
\int_0^t I_4(s) ds &= \int_0^t \left((\varepsilon - 1) \nabla \cdot \eta_s, \nabla \cdot \xi_s \right) ds = \int_0^t \left(\sqrt{\varepsilon - 1} \nabla \cdot \eta_s, \sqrt{\varepsilon - 1} \nabla \cdot \xi_s \right) ds \\
&\leq \int_0^t \|\nabla \cdot \eta_s\|_{\varepsilon-1}^2 ds + \frac{1}{4} \int_0^t \|\nabla \cdot \xi_s\|_{\varepsilon-1}^2 ds.
\end{aligned} \tag{72}$$

Note that due to the vanishing boundary condition, the contribution from the boundary is not present. This however can be inserted by considering a modified *triple* norm including, e.g., reflecting boundaries as in the case of Ω_{FEM} below. Hence, once again, a kick-back argument, with all ξ_s and ξ_{ss} weighted-norms on the left hand side are hidden in the corresponding terms in $[\|\xi_t\|]_{\varepsilon}^2$ giving the η_t estimate (65) for ξ_t , which, combined with (64), gives the desired result. \square

6.2 Error estimates: SD problem in Ω_{FEM}

The estimates here are mostly the same as those of their previous subsection. However, here we have a reflexive boundary condition on $\partial\Omega_{FEM}$. Hence, the estimates contain an extra contribution from the boundary (in the previous subsection, we have only considered the zero boundary condition for the whole Ω). Here, we include the procedure containg boudary term estimates, which can be mimiked in the case of the reflexive boundary condition in whole Ω .

Theorem

Let $E \in \mathbf{W}^2(\Omega_{FEM})$ and consider the continuous piecewise polynomial approximation for the solution of the problem (15). Furthermore, assume that $f_1 \in L_{2,\varepsilon}(\Omega_{FEM})$, $f_0 \in H^1(\Omega_{FEM}) \cap H_{\sqrt{\varepsilon}}^1(\Omega_{FEM}) \cap H_{\varepsilon-1}^1(\Omega_{FEM})$, and $g \in L_2(\partial\Omega_{FEM})$. Then there is a constant C such that

$$[\|e\|]_{\varepsilon, \Omega_{FEM}} \leq C_{\varepsilon}^t h. \tag{73}$$

Proof. Following the same procedure as the error estimates in Ω , and letting now

$$(E - E_h)_{\Omega_{FEM}} := (E - \tilde{E}_h)_{\Omega_{FEM}} + (\tilde{E}_h - E_h)_{\Omega_{FEM}} := \rho + \theta, \tag{74}$$

we need to estimate a triple norm of the form

$$\begin{aligned}
[\|E - E_h\|]_{\varepsilon, \Omega_{FEM}}^2 &:= \|\partial_t(E - E_h)\|_{\varepsilon, \Omega_{FEM}}^2 + \|\nabla(E - E_h)\|_{\Omega_{FEM}}^2 \\
&+ \|E - \tilde{E}_h\|_{|\nabla\varepsilon|, \Omega_{FEM}}^2 + \|\nabla \cdot (E - E_h)\|_{|\nabla\varepsilon| + \varepsilon - 1, \Omega_{FEM}}^2 \\
&+ \int_0^t \|\partial_t(E - E_h)\|_{\partial\Omega_{FEM}}^2(s) ds + \int_0^t \|g - g_h\|_{\partial\Omega_{FEM}}^2(s) ds.
\end{aligned} \tag{75}$$

Assuming that, at the boundary $\partial\Omega$, g is as regular as E , the linear interpolation error reads:

$$[\|\rho\|]_{\varepsilon, \Omega_{FEM}}(t) \sim C_{\varepsilon}^t h_{\Omega_{FEM}}, \tag{76}$$

Then following the same procedure as above we have for both (16) and its continuous version, and with $\zeta = E$ and $\zeta = E_h$ corresponding to $G = g$, and $G = g_h$, respectively, we have

$$\begin{aligned} B_{\Omega_{FEM}}(\zeta, \mathbf{v}) &:= (\varepsilon \partial_{tt} \zeta, \mathbf{v}) + (\nabla \zeta, \nabla \mathbf{v}) + ((\nabla \varepsilon) \cdot \zeta, \nabla \cdot \mathbf{v}) - ((\varepsilon - 1) \nabla \cdot \zeta, \nabla \cdot \mathbf{v}) \\ &= \langle G, \mathbf{v} \rangle_{\partial \Omega_{FEM}}, \quad \forall \mathbf{v} \in \mathbf{W}_h^E(\Omega_{FEM}). \end{aligned} \quad (77)$$

with the associated data. Hence we can write

$$\begin{aligned} B_{\Omega_{FEM}}(\theta, \theta) &= B_{\Omega_{FEM}}(\tilde{E}_h - E_h, \theta) \\ &\quad - B_{\Omega_{FEM}}(E - \tilde{E}_h, \theta) + B_{\Omega_{FEM}}(E - \tilde{E}_h, \theta) \\ &= -B_{\Omega_{FEM}}(e, \theta) + B_{\Omega_{FEM}}(\rho, \theta) \\ &= \langle g_h - g, \theta \rangle_{\partial \Omega_{FEM}} + B_{\Omega_{FEM}}(\rho, \theta). \end{aligned} \quad (78)$$

In the triple norm form this yields

$$\begin{aligned} [|\theta|]_{\varepsilon, \Omega_{FEM}}^2(t) &= [|\tilde{E}_h - E_h|]_{\varepsilon, \Omega_{FEM}}^2(t) \leq C_\varepsilon^t \int_0^t B_{\Omega_{FEM}}(\theta, \theta) ds \\ &= \int_0^t \langle g_h - g, \theta \rangle_{\partial \Omega_{FEM}} ds + \int_0^t B_{\Omega_{FEM}}(\rho, \theta) ds \\ &\leq \int_0^t |g - g_h|_{\partial \Omega_{FEM}}^2 ds + \frac{1}{4} \int_0^t |\theta|_{\partial \Omega_{FEM}}^2 ds \\ &\quad + [|\rho|]_{\varepsilon, \Omega_{FEM}}^2(t) + \frac{1}{4} [|\theta|]_{\varepsilon, \Omega_{FEM}}^2(t). \end{aligned} \quad (79)$$

Now using the same procedure as in the proof of the previous theorem (with ξ and η replaced by ρ and θ) to bound all the involved norms and hiding both θ -terms on the right, inside $[|\theta|]_{\varepsilon, \Omega_{FEM}}^2(t)$, on the left hand side, together with estimates (76) for ρ , and further assuming corresponding estimates for $\langle g_h - g, \theta \rangle_{\partial \Omega_{FEM}}$, we obtain (omitting some details) that

$$[|\theta|]_{\varepsilon}^2(t) \leq (C_\varepsilon^t)^2 \left([|\rho|]_{\varepsilon}^2(t) + \int_0^t |\langle g_h - g, \theta \rangle_{\partial \Omega_{FEM}}|^2 ds \right). \quad (80)$$

Now (76) and (80) together with the corresponding estimates for $\langle g_h - g, \theta \rangle_{\partial \Omega_{FEM}}$, give the desired result and completes the proof. \square

7 Numerical examples

In this section we present numerical examples justifying theoretical results of the previous two sections. For convergence tests the domain decomposition algorithm (see Algorithm 2), implemented in the software package WavES [30], was used. We note that because of

Algorithm 2 Domain decomposition algorithm for solution of Maxwell's equations (2). At every time step k are performed the following operations:

- 1: Compute E^{k+1} in Ω_{FDM} using the explicit finite difference scheme (29) with known E^k , and E^{k-1} -values.
 - 2: Compute E^{k+1} in Ω_{FEM} by using the finite element scheme (22) with known E^k, E^{k-1} .
 - 3: For the finite difference method in Ω_{FDM} , use the values of the function E^{k+1} at nodes ω_\circ (green boundary of Figure 1), which are computed using the finite element scheme (24), as a boundary condition at the inner boundary of Ω_{FDM} .
 - 4: Apply appropriate boundary condition at the outer boundary of Ω_{FDM} .
 - 5: For the finite element method in Ω_{FEM} , use the values of the functions E^{k+1} at nodes ω_\circ (blue boundary of the Figure 1), which are computed using the finite difference scheme (29) as a boundary condition.
 - 6: Apply swap of the solutions for the computed function E^{k+1} to be able to perform the algorithm on a new time level k .
-

using explicit FE and FD schemes in Ω_{FEM} and Ω_{FDM} , correspondingly, we need to choose time step τ according to the CFL stability condition (7) derived in [5] so that the whole hybrid scheme remains stable.

Numerical tests are performed in time interval $(0, T) = (0, 0.25)$ and in the spatial dimensionless computational domain

$$\Omega = \{(x, y) : x \in [0, 1], y \in [0, 1]\}, \quad (81)$$

which is split into the finite element domain

$$\Omega_{FEM} = \{(x, y) : x \in [0.25, 0.75], y \in [0.25, 0.75]\} \quad (82)$$

and the finite difference domain Ω_{FDM} , thus $\Omega = \Omega_{FEM} \cup \Omega_{FDM}$, see Figure 1.

The model problem in all our tests that is stated for the electric field $E = (E_1, E_2)$ is as follows:

$$\begin{aligned} \varepsilon \partial_{tt} E + \nabla(\nabla \cdot E) - \Delta E - \nabla \nabla \cdot (\varepsilon E) &= F && \text{in } \Omega \times (0, T), \\ E(\cdot, 0) = 0 \text{ and } \partial_t E(\cdot, 0) &= 0 && \text{in } \Omega, \\ E &= 0 && \text{on } \partial\Omega \times (0, T). \end{aligned} \quad (83)$$

We have the functions

$$\begin{aligned} E_1 &= \frac{1}{\varepsilon} 2\pi \sin^2 \pi x \cos \pi y \sin \pi y \frac{t^2}{2}, \\ E_2 &= -\frac{1}{\varepsilon} 2\pi \sin^2 \pi y \cos \pi x \sin \pi x \frac{t^2}{2}, \end{aligned} \quad (84)$$

as the exact solution $E = (E_1, E_2)$ of the model problem (83) with the source data $F = (F_1, F_2)$ which corresponds to this exact solution.

The function ε in (83) is defined as

$$\varepsilon(x, y) = \begin{cases} 1 + \sin^m \pi(2x - 0.5) \cdot \sin^m \pi(2y - 0.5) & \text{in } \Omega_{FEM}, \\ 1 & \text{in } \Omega_{FDM}. \end{cases} \quad (85)$$

We choose $m = 2, 4, 6, 8$ in our numerical examples, see Figure 2, for these functions in the domain Ω_{FEM} . We note that the exact solution (84) satisfies the divergence free condition $\nabla \cdot (\varepsilon E) = 0$ for ε defined by (85), the homogeneous initial conditions, as well as the homogeneous Dirichlet conditions for all times.

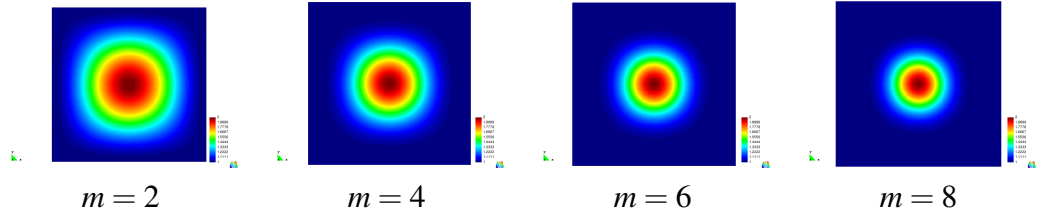


Figure 2: Function $\varepsilon(x, y)$ in the domain Ω_{FEM} for different values of m in (85).

The computational domain $\Omega_{FEM} \times (0, T)$ was discretized into triangular elements with mesh sizes $h_l = 2^{-l}$, $l = 3, 4, 5, 6$, and the mesh in $\Omega_{FDM} \times (0, T)$ was decomposed into squares of the same mesh sizes as described in Section 3, see Figure 1. The time step was chosen corresponding to the stability criterion (7) as $\tau_l = 0.025 \cdot 2^{-l}$ for $l = 3, 4, 5, 6$. Convergence results of the proposed finite element scheme computed in L_2 and H^1 norms are presented in Tables 2 - 4 for $m = 2, 4, 6, 8$ in (85). Relative norms in these tables were computed as

$$e_l^1 = \frac{\max_{1 \leq k \leq N} \|E^k - E_h^k\|}{\max_{1 \leq k \leq N} \|E^k\|}, \quad (86)$$

$$e_l^2 = \frac{\max_{1 \leq k \leq N} \|\nabla(E^k - E_h^k)\|}{\max_{1 \leq k \leq N} \|\nabla E^k\|}.$$

E and E_h are the exact and computed FE solutions in $\Omega_{FEM} \times (0, T)$, respectively, and $N = T/\tau_l$. Logarithmic convergence rates r_1, r_2 in these tables are computed, viz.

$$r_1 = \frac{\left| \log \left(\frac{e_h^1}{e_{2h}^1} \right) \right|}{|\log(0.5)|}, \quad \text{and} \quad r_2 = \frac{\left| \log \left(\frac{e_h^2}{e_{2h}^2} \right) \right|}{|\log(0.5)|}, \quad (87)$$

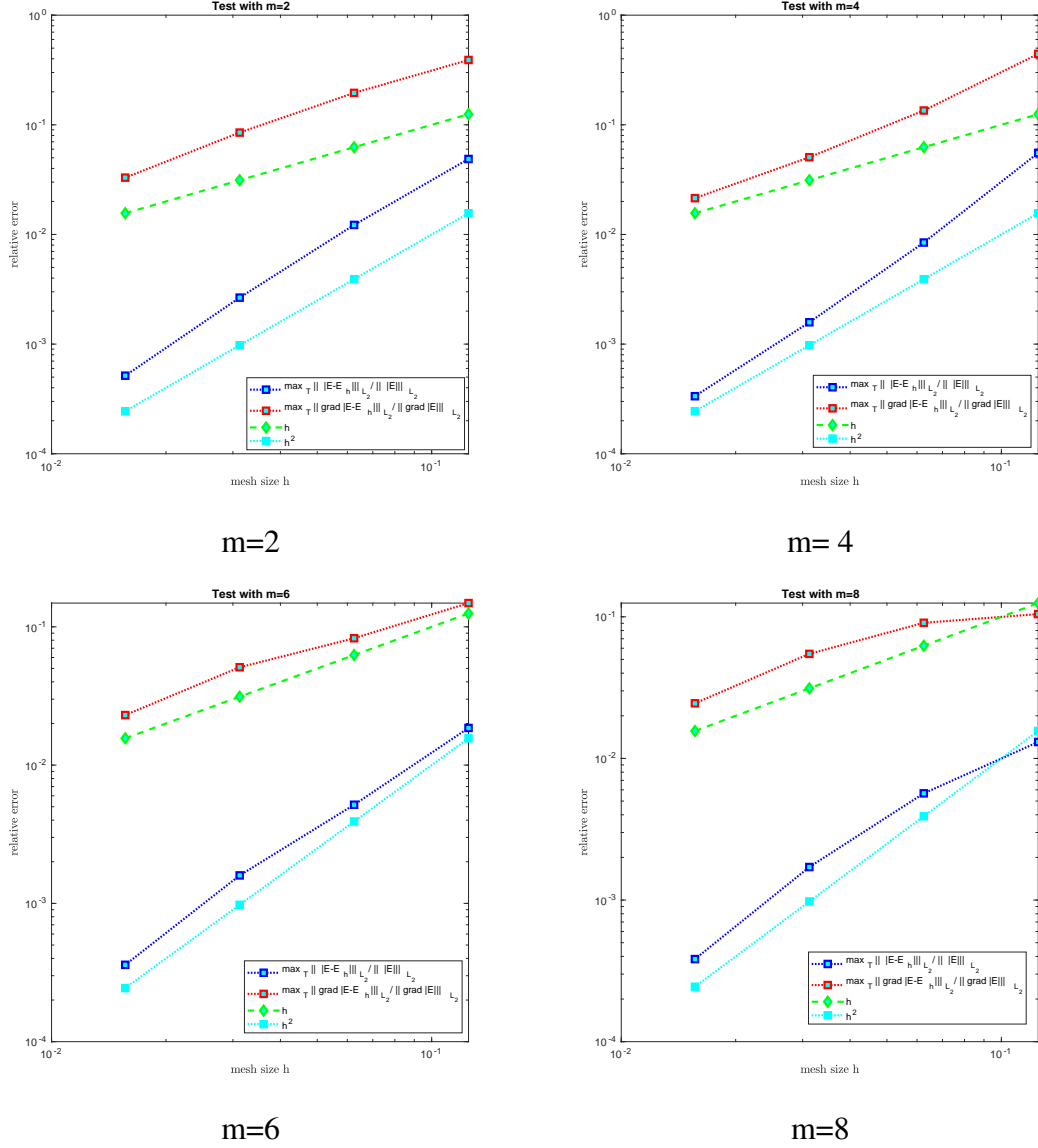


Figure 3: Convergence of the relative L_2 and H^1 norms computed via (86).

where $el_h^{1,2}, el_{2h}^{1,2}$ are relative norms computed via (86) on the mesh \mathcal{T}_h with the mesh size h and $2h$, respectively. Figure 3 shows convergence of the relative L_2 and H^1 norms computed

l	nel	nno	e_l^1	$\frac{e_l^1}{e_{2h}^1}$	r_1	e_l^2	$\frac{e_l^2}{e_{2h}^2}$	r_2
3	128	81	$4.878 \cdot 10^{-2}$	—	—	$3.902 \cdot 10^{-1}$	—	—
4	512	289	$1.222 \cdot 10^{-2}$	3.992	1.997	$1.955 \cdot 10^{-1}$	1.996	0.997
5	2048	1089	$2.654 \cdot 10^{-3}$	4.604	2.203	$8.492 \cdot 10^{-2}$	2.302	1.203
6	8192	4225	$5.15 \cdot 10^{-4}$	5.151	2.365	$3.297 \cdot 10^{-2}$	2.575	1.365

Table 1: Relative errors e_l^1 and e_l^2 in the L_2 - and H^1 -norms, respectively, for mesh sizes $h_l = 2^{-l}, l = 3, \dots, 6$, for $m = 2$ in (85).

l	nel	nno	e_l^1	$\frac{e_l^1}{e_{2h}^1}$	r_1	e_l^2	$\frac{e_l^2}{e_{2h}^2}$	r_2
3	128	81	$5.54 \cdot 10^{-2}$	—	—	$4.432 \cdot 10^{-1}$	—	—
4	512	289	$8.438 \cdot 10^{-3}$	6.565	2.7148	$1.35 \cdot 10^{-1}$	3.283	1.715
5	2048	1089	$1.581 \cdot 10^{-3}$	5.337	2.4160	$5.06 \cdot 10^{-2}$	2.668	1.416
6	8192	4225	$3.35 \cdot 10^{-4}$	4.722	2.2394	$2.143 \cdot 10^{-2}$	2.361	1.239

Table 2: Relative errors e_l^1 and e_l^2 in the L_2 -norm and in the H^1 -norm, respectively, for mesh sizes $h_l = 2^{-l}, l = 3, \dots, 6$, for $m = 4$ in (85).

l	nel	nno	e_l^1	$\frac{e_l^1}{e_{2h}^1}$	r_1	e_l^2	$\frac{e_l^2}{e_{2h}^2}$	r_2
3	128	81	$1.856 \cdot 10^{-2}$	—	—	$1.485 \cdot 10^{-1}$	—	—
4	512	289	$5.168 \cdot 10^{-3}$	3.592	1.845	$8.268 \cdot 10^{-2}$	1.796	0.778
5	2048	1089	$1.594 \cdot 10^{-3}$	3.243	1.697	$5.099 \cdot 10^{-2}$	1.621	0.697
6	8192	4225	$3.6 \cdot 10^{-4}$	4.432	2.148	$2.301 \cdot 10^{-2}$	2.216	1.148

Table 3: Relative errors e_l^1 and e_l^2 in the L_2 -norm and in the H^1 -norm, respectively, for mesh sizes $h_l = 2^{-l}, l = 3, \dots, 6$, for $m = 6$ in (85).

l	nel	nno	e_l^1	$\frac{e_l^1}{e_{2h}^1}$	r_1	e_l^2	$\frac{e_l^2}{e_{2h}^2}$	r_2
3	128	81	$1.131 \cdot 10^{-2}$	—	—	$1.045 \cdot 10^{-1}$	—	—
4	512	289	$5.669 \cdot 10^{-3}$	2.304	1.204	$9.071 \cdot 10^{-2}$	1.152	0.2
5	2048	1089	$1.711 \cdot 10^{-3}$	3.314	1.728	$5.475 \cdot 10^{-2}$	1.657	0.728
6	8192	4225	$3.83 \cdot 10^{-4}$	4.468	2.16	$2.451 \cdot 10^{-2}$	2.234	1.16

Table 4: Relative errors e_l^1 and e_l^2 in the L_2 -norm and in the H^1 -norm, respectively, for mesh sizes $h_l = 2^{-l}, l = 3, \dots, 6$, for $m = 8$ in (85).

via (86) and compared with exact behavior of h and h^2 .

Computed hybrid FE/FD versus exact solutions with $m = 8$ in (85) at the time $t = 0.25$ are presented in Figures 4, where $|E_h|$ is computed using the domain decomposition algo-

rithm (Algorithm 2) for different meshes with sizes $h_l = 2^{-l}, l = 3, 4, 5, 6$. The top figures of Figure 4 present hybrid FE/FD meshes which were used for computations; common hybrid FE/FD solution in Ω is presented in the middle figures, and bottom figures show only FD solution as the part of the common hybrid solution in Ω_{FDM} . Interpreting these figures we observe smooth behavior of the hybrid solution across finite element/finite difference boundary, as was predicted in theory.

Furthermore, through these figures, as well as tables and Figure 3, we observe that with increasing l in $h_l = 2^{-l}, l = 3, 4, 5, 6$, the computational errors approach the second order convergence in L_2 - and first order in H^1 -norm for $m = 2, 4, 6, 8$. Therefore, we can conclude that the finite element scheme in the hybrid FE/FD method; considered in Ω_{FEM} , behaves like a first order method in H^1 -norm and a second order method in the L_2 -norm. These results are all in good agreement with the analytic estimates derived in Sections 5-6, as well as with results presented for finite element method in [5, 6] for the whole Ω .

Conclusion

In this paper we present stability and convergence analysis for the domain decomposition FE/FD method for time-dependent Maxwell's equations developed in [2, 3]. The convergence is optimal due to the assumed maximal available regularity of the exact solution in a Sobolev space.

The analysis are performed for the semi-discrete (spatial discretization) problem for, the constructed, finite element schemes in two different settings: in Ω and Ω_{FEM} . The temporal discretization algorithms are constructed using the CFL condition (7) derived in [5]. We have implemented several numerical examples that validate the robustness of the theoretical studies.

In a forthcoming, complementary, study we plan to extend the results in here to a problem with the presence of electrical conductivity term $\sigma \partial_t E$ which renders the equation to an parabolic-hyperbolic one.

Acknowledgments

The research of both authors is supported by the Swedish Research Council grant VR 2018-03661. The first author acknowledges the support of the VR grant DREAM.

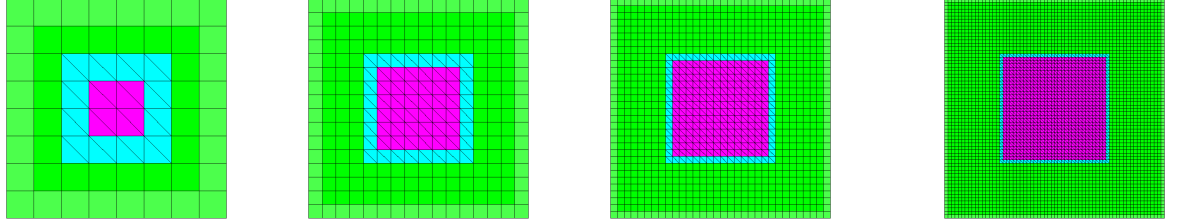
References

- [1] L. Beilina, Application of the finite element method in a quantitative imaging technique, *J. Comput. Methods Sci. Eng.*, IOS Press, 16(4), 755-771, 2016. DOI 10.3233/JCM-160689.

- [2] L. Beilina, M. Grote, Adaptive Hybrid Finite Element/Difference method for Maxwell's equations, *TWMS Journal of Pure and Applied Mathematics*, 1 (2) s. 176-197, 2010.
- [3] L. Beilina, Energy estimates and numerical verification of the stabilized Domain Decomposition Finite Element/Finite Difference approach for time-dependent Maxwell's system, *Cent. Eur. J. Math.*, **11** (2013), 702-733 DOI: 10.2478/s11533-013-0202-3.
- [4] L. Beilina, Domain decomposition finite element/finite difference method for the conductivity reconstruction in a hyperbolic equation, *Communications in Nonlinear Science and Numerical Simulation*, Elsevier, 2016, doi:10.1016/j.cnsns.2016.01.016
- [5] L. Beilina, V. Ruas, Convergence of Explicit P1 Finite-Element Solutions to Maxwell's Equations, *Springer Proceedings in Mathematics and Statistics*, vol 328. Springer, Cham (2020)
- [6] L. Beilina, V. Ruas, An explicit P1 finite element scheme for Maxwell's equations with constant permittivity in a boundary neighborhood, arXiv:1808.10720v4
- [7] L. Beilina, N. T. Thánh, M. Klibanov, and J. B. Malmberg, Reconstruction of shapes and refractive indices from blind backscattering experimental data using the adaptivity, *Inverse Problems*, 30 (2014), 105007.
- [8] L. Beilina, N. T. Thánh, M.V. Klibanov and J. B. Malmberg, Globally convergent and adaptive finite element methods in imaging of buried objects from experimental backscattering radar measurements, *Journal of Computational and Applied Mathematics*, Elsevier, DOI: 10.1016/j.cam.2014.11.055, 2015.
- [9] J. Bondestam Malmberg, L. Beilina, An Adaptive Finite Element Method in Quantitative Reconstruction of Small Inclusions from Limited Observations, *Appl. Math. Inf. Sci.*, 12(1), 1-19, 2018.
- [10] G. C. Cohen, *Higher Order Numerical Methods for Transient Wave Equations*, Springer-Verlag, Berlin, 2002.
- [11] T. Chan and T. Mathew, Domain decomposition algorithms, In A. Iserles, editor, *Acta Numerica*, 3, Cambridge University Press, Cambridge, 1994.
- [12] F. Edelvik, U. Andersson and G. Ledfelt, (2000), Explicit hybrid time domain solver for the Maxwell equations in 3D, AP2000 Millennium Conference on Antennas & Propagation, Davos.
- [13] A. Elmkies and P. Joly, Finite elements and mass lumping for Maxwell's equations: the 2D case. *Numerical Analysis*, C. R. Acad.Sci.Paris, 324, pp. 1287–1293, 1997.
- [14] B. Jiang, *The Least-Squares Finite Element Method. Theory and Applications in Computational Fluid Dynamics and Electromagnetics*, Springer-Verlag, Heidelberg, 1998.

- [15] B. Jiang, J. Wu and L. A. Povinelli, The origin of spurious solutions in computational electromagnetics, *Journal of Computational Physics*, 125, pp.104–123, 1996.
- [16] J. Jin, *The finite element method in electromagnetics*, Wiley, 1993.
- [17] P. Joly, Variational methods for time-dependent wave propagation problems, Lecture Notes in Computational Science and Engineering, Springer, 2003.
- [18] G. Chavent, *Nonlinear Least Squares for Inverse Problems. Theoretical Foundations and Step-by-Step Guide for Applications*, Springer, New York, 2009.
- [19] C. Johnson and J. Pitkäranta, Analysis of a the discontinuous Galerkin method for linear hyperbolic equations, *Math. Comp.*, 46 (173), pp.1-26, 1986.
- [20] P. B. Monk, *Finite Element methods for Maxwell's equations*, Oxford University Press, 2003.
- [21] P. B. Monk and A. K. Parrott, A dispersion analysis of finite element methods for Maxwell's equations, *SIAM J.Sci.Comput.*, 15, pp.916–937, 1994.
- [22] C. D. Munz, P. Omnes, R. Schneider, E. Sonnendrucker and U. Voss, Divergence correction techniques for Maxwell Solvers based on a hyperbolic model, *Journal of Computational Physics*, 161, pp.484–511, 2000.
- [23] J.-C. Nédélec, Mixed finite elements in R³, *Numerische Mathematik*, 35 (1980), 315-341.
- [24] K. D. Paulsen, D. R. Lynch, Elimination of vector parasites in Finite Element Maxwell solutions, *IEEE Transactions on Microwave Theory Technologies*, 39, 395 –404, 1991.
- [25] T. Rylander and A. Bondeson, (2000), Stable FEM-FDTD hybrid method for Maxwell's equations, *J. Comput.Phys.Comm.*, 125.
- [26] T. Rylander and A. Bondeson, (2002), Stability of Explicit-Implicit Hybrid Time-Stepping Schemes for Maxwell's Equations, *J. Comput.Phys.*
- [27] N. T. Thánh, L. Beilina, M. V. Klibanov, and M. A. Fiddy, Reconstruction of the refractive index from experimental backscattering data using a globally convergent inverse method, *SIAMJ. Sci. Comput.*, 36 (2014), pp. B273-B293.
- [28] N. T. Thánh, L. Beilina, M. V. Klibanov, M. A. Fiddy, Imaging of Buried Objects from Experimental Backscattering Time-Dependent Measurements using a Globally Convergent Inverse Algorithm, *SIAM Journal on Imaging Sciences*, 8(1), 757-786, 2015.
- [29] A. Toselli and B. Widlund, *Domain Decomposition Methods*, Springer, Berlin, 2005.
- [30] Software package WavES at <http://www.waves24.com/>

Computational meshes in the domain decomposition of $\Omega = \Omega_{\text{FEM}} \cup \Omega_{\text{FDM}}$



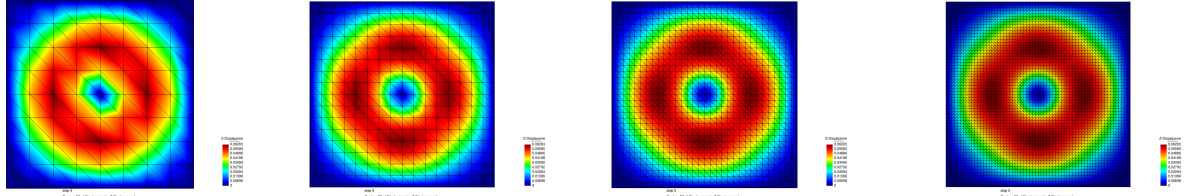
$h = 0.125$

$h = 0.0625$

$h = 0.03125$

$h = 0.015625$

Exact solution $|E|, m = 8$, in Ω



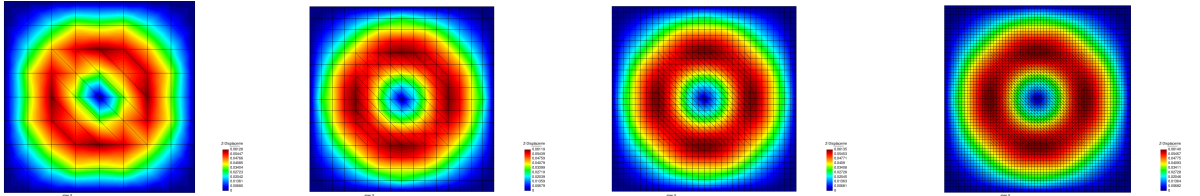
$h = 0.125$

$h = 0.0625$

$h = 0.03125$

$h = 0.015625$

Computed domain decomposition solution $|E_h|, m = 8$, in $\Omega = \Omega_{\text{FEM}} \cup \Omega_{\text{FDM}}$



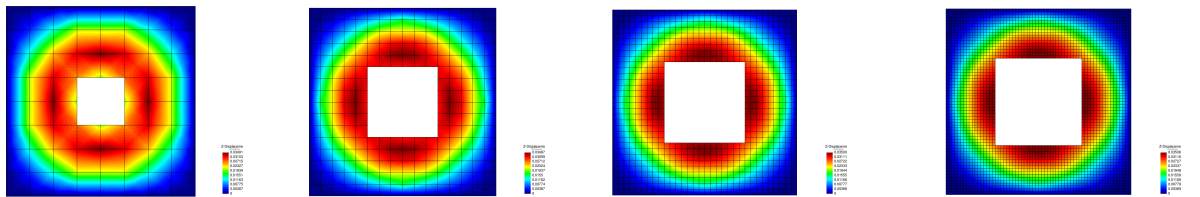
$h = 0.125$

$h = 0.0625$

$h = 0.03125$

$h = 0.015625$

Computed finite difference solution $|\hat{E}_h|, m = 8$, in the domain decomposition algorithm in Ω_{FDM}



$h = 0.125$

$h = 0.0625$

$h = 0.03125$

$h = 0.015625$

Figure 4: *Computed vs. exact solution at the time $t = 0.25$ for different meshes taking $m = 8$ in (85). Algorithm 2 was used in the domain decomposition method. Common elements in Ω_{FEM} and Ω_{FDM} on different meshes are presented on the top figures and are outlined by light blue color. We observe smooth hybrid solution across FE/FD boundaries.*